RISØ

Risø-R-894(EN)

Dose Rates from a C-14 Source using Extrapolation Chamber and MC Calculations

Jette Borg

Risø National Laboratory, Roskilde, Denmark
May 1996

Dose Rates from a C-14 Source using Extrapolation Chamber and MC Calculations

Risø-R-894(EN)

Jette Borg

Risø National Laboratory, Roskilde, Denmark
May 1996

Abstract The extrapolation chamber technique and the Monte Carlo (MC) calculation technique based on the EGS4 system have been studied for application for determination of dose rates in a low-energy β radiation field e.g., that from a ^{14}C source. The extrapolation chamber measurement method is the basic method for determination of dose rates in β radiation fields. Applying a number of correction factors and the stopping power ratio, tissue to air, the measured dose rate in an air volume surrounded by tissue equivalent material is converted into dose to tissue. Various details of the extrapolation chamber measurement method and evaluation procedure have been studied and further developed, and a complete procedure for the experimental determination of dose rates from a ^{14}C source is presented. A number of correction factors and other parameters used in the evaluation procedure for the measured data have been obtained by MC calculations.

The whole extrapolation chamber measurement procedure was simulated using the MC method. The measured dose rates showed an increasing deviation from the MC calculated dose rates as the absorber thickness increased. This indicates that the EGS4 code may have some limitations for transport of very low-energy electrons i.e., electrons with estimated energies less than $10 - 20$ keV.

MC calculations of dose to tissue were performed using two models: a cylindrical tissue phantom and a computer model of the extrapolation chamber. The dose to tissue in the extrapolation chamber model showed an additional buildup dose compared to the dose in the tissue model.

Calculations and experiments were performed at Ionizing Radiation Standards, Institute for National Measurement Standards, National Research Council of Canada, with guidance of D. W. O. Rogers and L. van der Zwan. The work is an integral part of the author's Ph. D. project.

ISBN 87-550-2180-8
ISSN 0106-2840

Grafisk Service · Risø · 1996

Contents

1 Introduction

The extrapolation chamber measurement method is the basic method for determination of dose rates in β radiation fields. The extrapolation chamber measures dose rate e.g., in air, which according to the Bragg-Gray formula can be converted into absorbed dose rate in the material surrounding the air cavity using the stopping power ratio, medium to air, $s_{m,a}$ (Sect. 2.3). If the cavity is surrounded by tissue-equivalent material, absorbed dose rate to tissue can be determined. In practice, a number of corrections have to be applied during various stages of the measurement due to differences between tissue and the material surrounding the air cavity, and because the Bragg-Gray conditions will be only more or less fulfilled for different chamber depths.

In particular for measurements in low-energy β radiation fields, corrections due to attenuation of the β particles in the chamber air volume, the entrance window material and the air mass between the source and the chamber window may become highly significant. Correction factors and evaluation procedures have been established previously for measurements in radiation fields from ^{147}Pm, ^{204}Tl and ^{90}Sr/^{90}Y sources [1, 2]. In this work, correction factors and evaluation procedures for measurements with extrapolation chamber have been further studied and developed for the establishment of a reliable measurement method for determination of dose rates from the radiation field of a ^{14}C source, which is a low-energy β emitter with a maximum β energy of 156 keV. In addition to electrons, the spectrum from the ^{14}C source also contains bremsstrahlung photons produced in the source construction material. The spectra from the source have previously been determined from measurements as well as Monte Carlo (MC) calculations [3].

Measurements were performed using extrapolation chambers set up at NRC (National Research Council of Canada) and at Risø. The extrapolation chamber built at NRC has a construction similar to the chamber used at Risø, which is manufactured by PTW, Germany. Both chambers are constructed from nearly tissue-equivalent materials e.g., polymethyl methacrylate (PMMA), and they are therefore suitable for the measurement of absorbed dose rate in tissue. The report discusses the various parameters and factors to be used for the measurements of dose rates from the ^{14}C source. Some of these have been evaluated by MC calculations. Data are presented from measurements of dose rates using different absorbers in front of the extrapolation chamber, and procedures for evaluation of the experimental data are discussed. In particular, it is discussed whether procedures previously used for evaluating depth-dose profiles from radiation from a ^{147}Pm source [2] are also usable for the ^{14}C source.

Parallel with the experimental work, MC calculations were performed to study the utility of this technique for dosimetry of low-energy β radiation fields. MC calculations were performed using the Monte Carlo code EGS4 (Electron Gamma Shower version 4) [4] with the electron-transport algorithm PRESTA (Sect. 2.2). A simplified model of the source configuration was used in the calculations to make them more efficient [3].

MC calculations have been used to evaluate some of the correction factors for the extrapolation chamber measuring procedure for the ^{14}C source (Sect. 3). Furthermore, the complete measurement procedure has been modelled for MC calculations to validate this method with experimental data, and to use it for analysing in detail specific areas of the extrapolation chamber method e.g., the measurement of depth-dose profiles in tissue. Also the dose in tissue directly was calculated by the MC method using a phantom model consisting of a tissue cylinder. Measured and calculated depth-dose distributions were compared, and the reasons for differences discussed (Sect. 4.2).

In skin dosimetry the dose at a depth of 7 mg cm^{-2} is of particular interest. A transmission factor for this depth has been evaluated from the calculated and measured dose rates (Sect. 4.3).

2 Methods and Procedures

2.1 The ^{14}C Source

The source used in this work is a quadratic (50 mm x 50 mm, 1.0 mm thick) sheet of PMMA with the ^{14}C radionuclides uniformly distributed throughout the PMMA. It was purchased from Amersham Company and has a quoted source strength Q_0 = 57 MBq. The half life of ^{14}C is 5730 years, so there is no need for correction due to decay since time of purchase. An emission rate of electrons was measured by Amersham to be $d\phi_{p,e}/dt = 1.5 \cdot 10^6$ electrons cm^{-2} min^{-1} (or $2.5 \cdot 10^4$ electrons cm^{-2} s^{-1}). This type of source is normally used for radiographic examination of paper and similar materials or for use as check sources for multichannel chromatogram analyzers [5]. A dose rate of about 2 μGy s^{-1} was measured with an extrapolation chamber without any absorbers in front of the entrance window and at a distance of 50 mm air from the source (Sect. 4).

The source is placed in a 1.0 mm deep recess in a 12 mm thick holder of PMMA. The source is fixed in the holder by a 1.0 mm thick PMMA sheet with a 50 mm diameter hole. The configuration of source and holder is shown in Fig. 1.

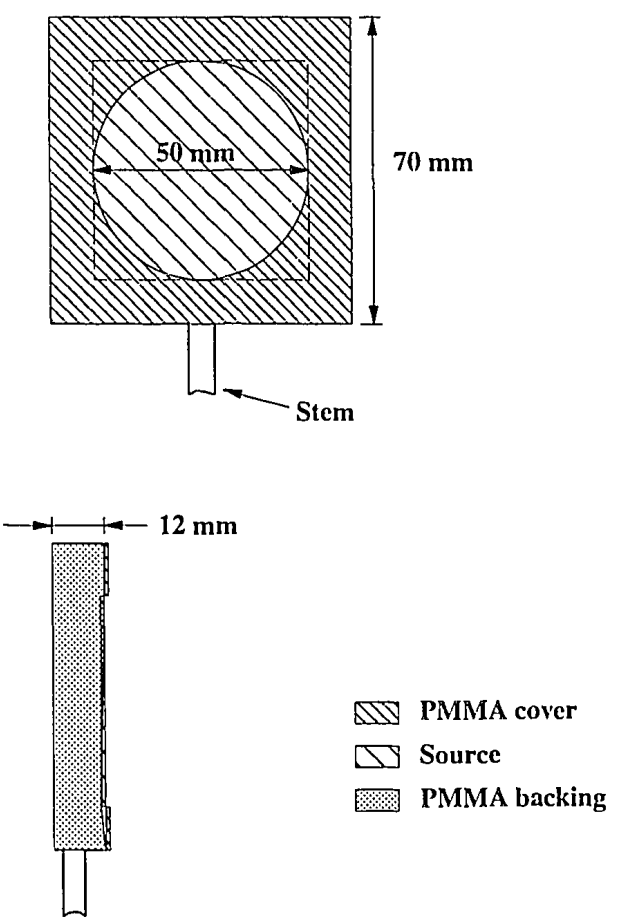

Figure 1. The configuration of the physical source including source holder (backing and cover) of PMMA.

All β particles emitted from the covered parts of the source are totally absorbed in the PMMA cover, which simplifies the MC modelling of the source to a cylindrical construction. However, due to production of bremsstrahlung from the covered

part of the source, these regions cannot be completely ignored in the calculations.

Since only a circular part of the source is used, the actual source strength, Q, is smaller than for the square source. The actual source strength being the number of β decays per second from the circular part of the source is obtained from

$$Q = Q_0 \cdot \pi \cdot (25 \text{ mm})^2/(50 \text{ mm})^2 = 45 \text{ MBq} \quad (1)$$

The planar fluence of electrons (simplified initial electrons), $\Phi_{p,e}$, at the source surface per source electron is then

$$\Phi_{p,e} = (\mathrm{d}\phi_{p,e}/\mathrm{d}t)/Q = 5.6 \cdot 10^{-4} \text{ simp. init. elec. cm}^{-2} \text{ per source elec.} \quad (2)$$

Assuming that no bremsstrahlung photons are created in the PMMA cover, the estimated ratio of photons from the physical source, $N_{ph.phys.}$, to photons from the modelled source, $N_{ph.mod.}$, is

$$N_{ph.phys.}/N_{ph.mod.} = \frac{(50 \text{ mm})^2}{\pi \cdot (25 \text{ mm})^2} = 1.27 \quad (3)$$

MC calculations of the electron and photon spectra on the source surface have been described previously [3]. In Fig. 2, these spectra are compared with the unmoderated spectrum for the ^{14}C nuclide. The electron spectra have been normalized to the peak values for comparison. It is obvious that the spectrum for the ^{14}C nuclide is modified when the β particles travel through the source material.

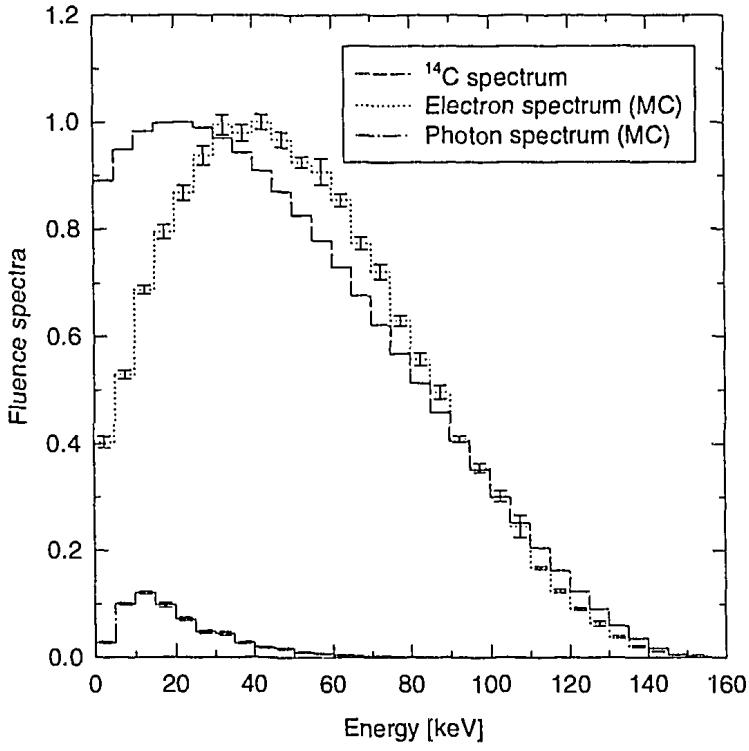

Figure 2. The spectrum for the ^{14}C radionuclide and the MC calculated fluence spectra for electrons and photons at the source surface shown in 5 keV bins. Average β energy for the radionuclide is 49 keV, and for the MC calculated spectra 52 keV for electrons and 22 keV for photons. The electron spectra are normalized to the peak values for comparison. The photon spectrum has been multiplied by the same normalization factor as the MC calculated electron spectrum.

2.2 Monte Carlo Calculations

The Monte Carlo code system EGS4 (Electron Gamma Shower version 4) [4] was used to calculate correction factors for the extrapolation chamber and to simulate the experiments with the extrapolation chamber. In the EGS4 code, the Parameter Reduced Electron-Step Transport Algorithm, PRESTA, was used in the simulations to avoid step-size artefacts [6]. The user codes FLURZ [7], DOSRZ [8] and SPRRZ [9] from the EGS4 system were used to calculate fluence, absorbed dose in tissue and stopping power ratio, medium to air, respectively, in regions of cylindrical geometry. The correlated sampling (CS) variance reduction technique (see below) was used to calculate the correction factors for the extrapolation chamber to be used for the evaluation of the measurement data. These correction factors were calculated as the ratios of absorbed doses in various geometries irradiated by photon and electron beams.

Calculations were performed at the NRC SGI R4400 computers, and calculation times stated in this report are for these computers. Energy cutoffs in the calculations were 512 keV for electrons (including the rest mass energy of an electron of 511 keV) and 1 keV for photons. In regions where an electron cannot return to regions of interest, the electron cutoff energy was 612 keV.

A simplified model of the source was used for the MC calculations. It consists of a disc of air with diameter 50 mm and thickness 1 μm, emitting electrons and photons isotropically. The electron and photon spectra on the source surface has been calculated by MC calculations [3] and were used as input spectra for the simplified source model.

The dose rate in the air of the extrapolation chamber (described in Sect. 2.3) was calculated using a complete model of the chamber with different filters in front of the entrance window. The dose rate to the air cavity, c, in the chamber at a distance of 50 mm from the source was calculated by using the simplified source model and by applying the normalization factor, F_{CS}, to correct for the difference in fluence at the detector position calculated when using the simplified source model instead of the complete model [3]. The dose rates, $\dot{D}_e$ and $\dot{D}_{ph}$, from electrons and photons, respectively, were calculated in Gy s^{-1} from the formulas

$$\begin{aligned}\dot{D}_e(d) &= Q \cdot F_{CS,e} \cdot D'_e(d) \\ &= Q \cdot (2.90 \cdot 10^{-2} \pm 2.5\,\%) \cdot D'_e(d) \\ &= (1.31 \cdot 10^{6} \pm 2.5\,\%) \cdot D'_e(d) \end{aligned} \quad (4)$$

and

$$\begin{aligned}\dot{D}_{ph}(d) &= Q \cdot F_{CS,ph} \cdot D'_{ph}(d) \\ &= Q \cdot (7.35 \cdot 10^{-4} \pm 3.4\,\%) \cdot D'_{ph}(d) \\ &= (3.31 \cdot 10^{4} \pm 3.4\,\%) \cdot D'_{ph}(d)\,, \end{aligned} \quad (5)$$

where $D'_e(d)$ and $D'_{ph}(d)$ are the calculated absorbed doses in Gy per simplified source electron for calculations with the simplified source model and d is the absorber thickness in mg cm^{-2}. $D'_{ph}(d)$ is the dose due to the bremsstrahlung photons generated in the source material. The source strength was assumed to be $Q = 45$ MBq. In the calculations of the dose rates, the calculated uncertainty does not include an uncertainty on the source strength.

The calculated dose rate to air is then

$$\begin{aligned}\dot{D}_{c,cal}(d) &= \dot{D}_e(d) + \dot{D}_{ph}(d) \\ &= (1.31 \cdot 10^{6} \pm 2.5\,\%) \cdot D'_e(d) + (3.31 \cdot 10^{4} \pm 3.4\,\%) \cdot D'_{ph}(d) \end{aligned} \quad (6)$$

Correlated Sampling

Correlated sampling can be applied to problems where the ratio or difference in certain quantities (e.g., absorbed dose) due to different geometries or media is of interest [10]. Instead of performing two independent simulations (uncorrelated) with the different geometries or media, the correlated sampling technique uses the similar particle trajectories for the estimation for both geometries and the respective estimates will be strongly correlated and are expected to deviate from their expectation values in the same direction. In Fig. 3, the method is visualized. *For the two situations the particles follow the same trajectories in region* 1 with medium A. Entering region 2 with medium A in one case and medium B in another, the particles follow different trajectories in the two cases. The ratio of the two estimates is then expected to have a smaller uncertainty than the corresponding ratio in the uncorrelated simulation. The calculation efficiency and accuracy increases with the degree of correlation between the calculated doses in similar thin-slab geometries.

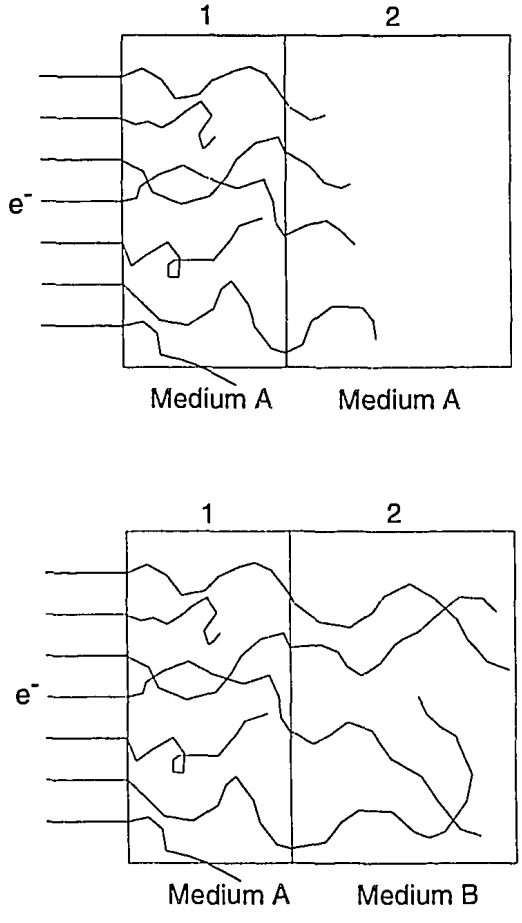

Figure 3. Correlated sampling technique. In region 1, the trajectories of the particles are the same for the two MC calculations. When particles enter region 2, they interact differently in the two media A and B.

In an earlier report [10] some limitations of the CS method have been pointed out: "If the electron angular and spatial distribution cannot be simulated properly, the chamber response is likely to be affected. This is a potentially serious limitation for nonspherical cavities, such as those in pancake-like or long cylindrical ionization chambers."

Since a simplified model of the source has been used in the calculations, the

electron angular and spatial distributions may not be exactly those of the real source. However, the spectra have been studied and compared. The conclusion was that the simplified source model could be used instead of an almost exact model of the source [3].

2.3 The Extrapolation Chamber

The extrapolation chamber measurement method is the basic method for determination of dose rates in β radiation fields. The extrapolation chamber measures dose rates e.g., in air, which according to the Bragg-Gray formula can be converted into absorbed dose rate in the material surrounding the air cavity using the stopping power ratio, medium to air, $s_{m,a}$. In practice, a number of corrections have to be applied during various stages of the measurement due to differences between tissue and the material surrounding the air cavity, and because the Bragg-Gray conditions will be only more or less fulfilled for different chamber depths.

The extrapolation chamber is an ionization chamber in which the distance between the entrance window and the collector electrode can be varied i.e., the chamber volume is variable. In Fig. 4, the extrapolation chamber used at NRC is seen with the ^{14}C source in front of it.

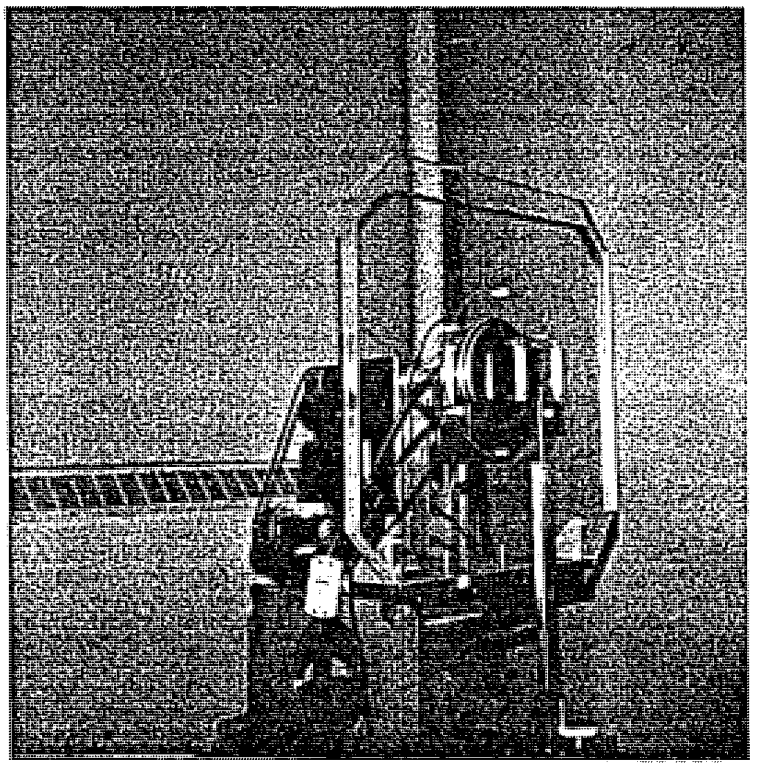

Figure 4. The extrapolation chamber set-up at NRC. The ^{14}C source is placed in front of the extrapolation chamber.

The extrapolation chamber model used in the MC calculations is shown in Fig. 5. It is similar to the extrapolation chamber at NRC, though screws and connectors have been simplified to PMMA in the MC model.

The entrance window is a 3.4 μm thick graphite coated mylar foil of total thickness (0.954 $\pm$ 0.095) mg cm^{-2} [11]. The collecting electrode has an effective area of (7.093 $\pm$ 0.005) cm^2, is made of PMMA and has a graphite coating 0.480 mg cm^{-2} thick. Also the sidewall is made of PMMA. The electrical field strength in each measurement is 10^4 V m^{-1}. The extrapolation chamber is connected to a

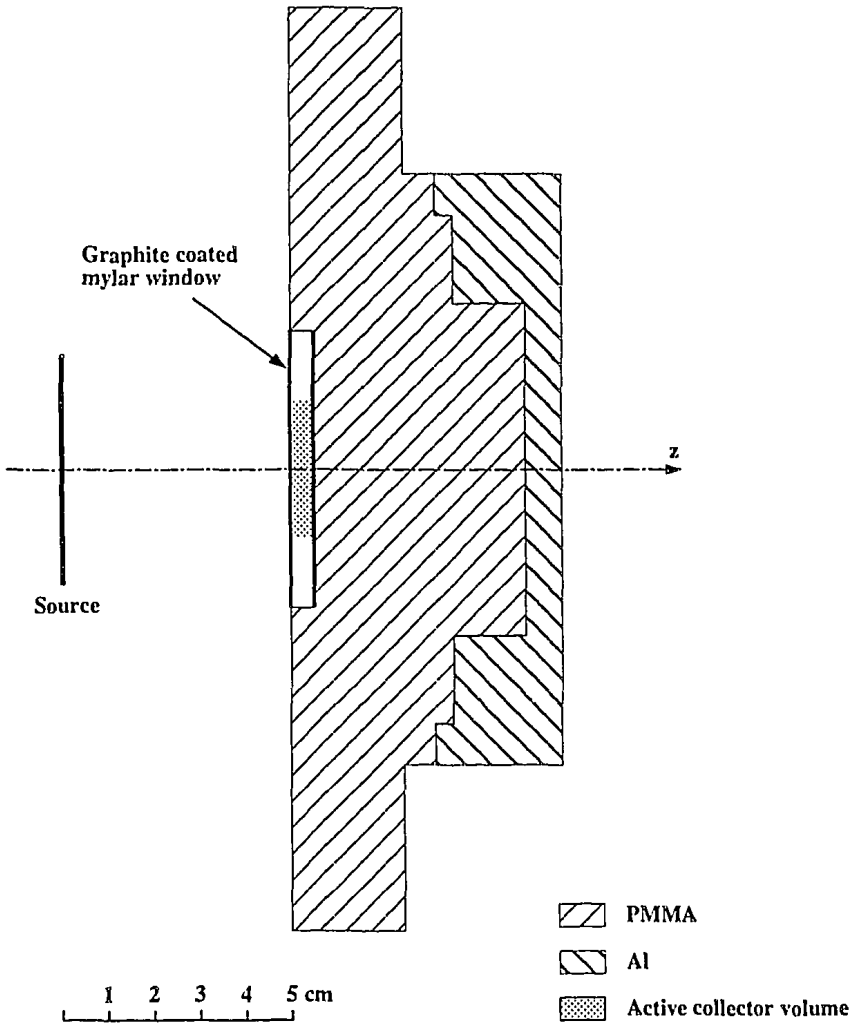

Figure 5. Extrapolation chamber configuration in MC calculations. It is similar to the extrapolation chamber used at NRC, though screws and connectors have been simplified to PMMA in the MC model.

Keithley 642 remote head and electrometer. The extrapolation chamber used at Riso is similar to the one from NRC. However, the entrance window has a total thickness of 0.66 mgcm^{-2} mylar (equivalent to 0.62 mgcm^{-2} tissue when using the relative attenuation factors [12]) and the effective area of the collecting electrode is (7.16 ± 0.02) cm^2.

The measured quantity is the collected charge per second (= current I) as a function of the air mass in the collector volume, which is proportional to the chamber depth l [μm]. The current, I, was measured with both positive (I_+) and negative (I_-) chamber voltages to eliminate the polarity effect, though it is only a small effect for ^{14}C irradiations. Leakage current is also eliminated by measuring with positive and negative voltage as long as it is constant during both measurements. Under the assumption that polarity effect and leakage current do not change with the polarity of the chamber voltage, the difference between I_+ and I_- will be twice the ionization current, but corrected due to lack of saturation resulting from volume recombination (f_v), initial recombination (f_i), and diffusion loss (f_d). The ionization current, I, is determined using the collection efficiency f [1]:

$$I = (I_+ - I_-)/(2 \cdot f) \,, \tag{7}$$

where f is

$$f = f_v \cdot f_i \cdot f_d \tag{8}$$

and

$$f_v = 1 - \Gamma_0^2 \cdot l^4 \cdot q_m \cdot U^{-2} \tag{9}$$

$$f_i = 1 - E_1 \cdot l \cdot U^{-1} \tag{10}$$

$$f_d = 1 - 2 \cdot k^* \cdot T \cdot e^{-1} \cdot U^{-1} \ , \tag{11}$$

where
$\Gamma_0^2 = (5.05 \pm 0.25) \cdot 10^{13}$ V^2 A^{-1} m^{-1}
l = chamber depth
q_m = measured ionization rate (collected charge per volume and time)
$= (I_+ - I_-)/(2 \cdot a \cdot l)$
a = effective collector area
U = collecting voltage (absolute value)
$E_1 = 4.4$ V m^{-1}
e = elementary charge
T = air temperature (in K)
k^* = Boltzmann constant
$2 \cdot k^* \cdot T \cdot e^{-1} = 0.0505$ V at $T = 293.15$ K

If $I \leq 10^4$ fA, $U/l = 10^{-2}$ V μ^{-1}m and $a \approx 7.2 \cdot 10^{-4}$ m^2, it can be evaluated that $f \approx C = 1 - 0.0505 \cdot U^{-1} = 1 - 5.05 \cdot l^{-1}$ (l in μm), i.e.,

$$1/f \approx l/(l - 5.05) \tag{12}$$

The current, I_{cor} (corrected due to deviation from reference air conditions (see Sect. 3.1)), is obtained for chamber depths up to 2400 μm with intervals of 200 μm, and from these data the value of $(\mathrm{d}(I_{cor})/\mathrm{d}l)_{l \to 0}$ (see Eq. (17)) is found by fitting the data to a second order polynomial [2]:

$$I_{cor}(l) = a + b \cdot l + c \cdot l^2 \tag{13}$$

The fit is performed with the weight

$$w = 1/(l \cdot (s^2 + u^2)) \ , \tag{14}$$

where s and u are type A and type B uncertainties (see App. A). The chamber depth, l, is included in the weighting procedure because the Bragg-Gray conditions are best fulfilled for small chamber depths.

By extrapolating the curve to $l = 0$, the value of the charge collected per second per μm just behind the window is found.

$$\left(\frac{\mathrm{d}I_{cor}(l)}{\mathrm{d}l}\right)_{l \to 0} = b \tag{15}$$

From the value of $(\mathrm{d}I_{cor}(l)/\mathrm{d}l)_{l \to 0}$, the absorbed dose rate in the air in the chamber volume, $\dot{D}_c$, at a depth, d (total thickness of entrance window and added absorber in mg cm^{-2}), at reference air conditions is evaluated from

$$\dot{D}_c(d) = \left(\frac{W}{e}\right) \cdot \frac{k_{de}}{a \cdot \rho_{ref}} \cdot \left(\frac{\mathrm{d}(I_{cor})}{\mathrm{d}l}\right)_{l \to 0} \tag{16}$$

By multiplying by the stopping power ratio, tissue to air, $s_{t,a}$, and the correction for backscatter difference between tissue and back wall material, k_{bak}, the absorbed dose rate in tissue can be obtained from

$$\dot{D}_t(d) = s_{t,a} \cdot \left(\frac{W}{e}\right) \cdot \frac{k_{bak} \cdot k_{de}}{a \cdot \rho_{ref}} \cdot \left(\frac{\mathrm{d}(I_{cor})}{\mathrm{d}l}\right)_{l \to 0} \ , \tag{17}$$

where

$$I_{cor} = k \cdot I \tag{18}$$

and

$$k' = k \cdot k_{sw} = k_{pT} \cdot k_{sda} \cdot k_{hum} \cdot k_{sdh} \cdot k_{sw} \quad \text{(NRC)} \tag{19}$$

or

$$k' = k \cdot k_{sw} = k_{ad} \cdot k_{ab} \cdot k_{sw} \quad \text{(Risø)} \tag{20}$$

k_{bak}: correction for backscatter difference between tissue and back wall material
k_{de}: correction for source decay
k_{pT}: correction for air density (temperature and pressure) in chamber
k_{sda}: correction for air density (temperature and pressure) between source and detector
k_{hum}: correction for humidity in chamber
k_{sdh}: correction for humidity between source and detector
k_{ad}: correction for air density deviation (temperature, pressure and humidity) from reference air density
k_{ab}: correction for the absorption and scattering of β rays between source and detector
k_{sw}: correction for sidewall effect
W: the average energy required to produce an ion pair in air
e: the elementary charge
a: the effective collector area of the measuring volume of the extrapolation chamber
ρ_{ref}: the air density at reference air conditions

To obtain the dose rate to tissue, $\dot{D}_t(0)$, at the surface of the entrance window, a correction factor, k_{win}, is applied. k_{win} is the correction for the scattering and stopping of β rays in the entrance window and is applied only for measurements performed without any absorber in front of the entrance window.

$$\dot{D}_t(0) = k_{win} \cdot \dot{D}_t(d_w) \,, \tag{21}$$

where d_w is the window thickness.

Current Measurement at NRC

Repeated measurements of the charge collected in very short time-intervals (400 ms = internal frequency of the Keithley electrometer) during one current measurement has the advantage that the background current and the current without the shutter in front of the source can be measured in a well defined time i.e., the starting and ending time of the irradiation is well defined. This may be important for relatively short-time measurements, but does not matter for measurements of several minutes duration. In these experiments no shutter was used. The uncertainty (1 st. dev.) on one current measurement was calculated by use of the data obtained in the 400 ms intervals.

The current was measured at chamber depths ranging from 600 to 2400 μm with intervals of 200 μm and with both positive and negative chamber voltage.

Current Measurement at Risø

At Risø the collected charge was measured in time intervals of 200 to 2000 s duration depending on the absorber thickness. At each chamber depth from 400 to 2400 μm with intervals of 200 μm, the current was measured 5 times with positive and 5 times with negative chamber voltage. The standard deviation of the mean was calculated from these results.

3 Correction Factors and Stopping Power

In this chapter a number of correction factors and parameters used in Eqs. (17) and (21) in Sect. 2.3, to evaluate the dose rate to tissue from the measured current data, are discussed.

3.1 Correction for Changes in Air Conditions

As the measured current depends on the air density, it is necessary to correct all measured current data to represent the current at reference air conditions. Reference conditions used are temperature $T_{ref} = 293.15$ K, pressure $p_{ref} = 101.325$ kPa and relative humidity $r_{ref} = 45$ %. The density of air at reference conditions is $\rho_{ref} = 1.1995$ kg m^{-3} [13].

At NRC four correction factors for changes in air density from reference conditions were used. Between the source and the detector surface the absorption and scattering in the air is corrected for by the two factors, k_{sda} and k_{sdh}. In the collector volume in the extrapolation chamber the correction factors are k_{pT} and k_{hum}. The factors k_{sda} and k_{pT} corrects for the change in pressure and temperature, and k_{sdh} and k_{hum} for change in humidity. The air density as a function of humidity is given by the expression:

$$\rho(r) \simeq \rho_0 \cdot (1 - 0.3780 \cdot \left(\frac{p_{sv}}{p}\right) \cdot r) \ , \tag{22}$$

where ρ_0 is the air density at $r = 0$, r is the relative humidity $(0 - 1)$, and p_{sv} is the saturation vapour pressure of water, which is a function of air temperature and has the values 2.34 kPa at 20 °C and 2.64 kPa at 22 °C [14].

The correction factors are calculated through following equations:

$$k_{pT} = \frac{\rho_{ref}}{\rho(p,T)} = \frac{p_{ref} \cdot T}{p \cdot T_{ref}} \tag{23}$$

$$k_{hum} = \frac{\rho_{ref}}{\rho(r)} \simeq \frac{0.996}{1 - 0.3780 \cdot \frac{p_{sv}}{p} \cdot r} \tag{24}$$

k_{hum} was assumed constant and equal to 1.0.

Let $(\frac{\mu_{abs}}{\rho})_{air}$ be the mass absorption coefficient in air and R_{air} be the distance in air between source and detector. The correction for change in absorption between source and detector due to changes in pressure and temperature, assuming that $(\frac{\mu_{abs}}{\rho})_{air}$ has practically the same value for penetration depth $(R_{air} \cdot \rho_{ref})$ as for $(R_{air} \cdot \rho)$, is then obtained from

$$k_{sda} = \exp[-\left(\frac{\mu_{abs}}{\rho}\right)_{air} \cdot R_{air} \cdot (\rho_{ref} - \rho(p,T))] \tag{25}$$

$$\Downarrow$$

$$k_{sda} = A \cdot \exp(B \cdot \frac{p}{T}) \ , \tag{26}$$

where

$$A = \exp[-\left(\frac{\mu_{abs}}{\rho}\right)_{air} \cdot R_{air} \cdot \rho_{ref}] \tag{27}$$

and

$$B = \left(\frac{\mu_{abs}}{\rho}\right)_{air} \cdot R_{air} \cdot \rho_{ref} \cdot \frac{T_{ref}}{ref} \tag{28}$$

Similarly, the correction for change in absorption between source and detector due to change in humidity is obtained from

$$k_{sdh} = \exp[-\left(\frac{\mu_{abs}}{\rho}\right)_{air} \cdot R_{air} \cdot (\rho_{ref} - \rho(r))] \tag{29}$$

$$\Downarrow$$

$$k_{sdh} = \exp[-\left(\frac{\mu_{abs}}{\rho}\right)_{air} \cdot R_{air} \cdot \rho_{ref} \cdot (0.3780 \cdot r \cdot \frac{p_{sv}}{p} - 0.004)] \tag{30}$$

$$\Downarrow$$

$$k_{sdh} = C \cdot \exp(D \cdot r) \ , \tag{31}$$

where

$$C = \exp[\left(\frac{\mu_{abs}}{\rho}\right)_{air} \cdot R_{air} \cdot \rho_{ref} \cdot 0.004] \tag{32}$$

and

$$D = -\left(\frac{\mu_{abs}}{\rho}\right)_{air} \cdot R_{air} \cdot \rho_{ref} \cdot 0.3780 \cdot \frac{p_{sv}}{p} \tag{33}$$

The four coefficients A, B, C and D were calculated using a value of $(\frac{\mu_{abs}}{\rho})_{air} = 0.252\ \mathrm{cm^2 mg^{-1}}$ (see Table 1 in Sect. 3.2), a fixed distance of $R_{air} = 5.0$ cm, a value of $\rho_{ref} = 1.1995\ \mathrm{kg\,m^{-3}}$, and a value of $\frac{p_{sv}}{p} = 0.0231$, resulting in the correction coefficients

$$k_{sda} = 0.221 \cdot \exp(4.37 \cdot \frac{p}{T}) \tag{34}$$

and

$$k_{sdh} = 1.006 \cdot \exp(-1.32 \cdot 10^{-2} \cdot r) \tag{35}$$

The total correction, k_{ab}, for the air change from reference conditions between the source and the detector can then be written as

$$k_{ab} = k_{sda} \cdot k_{sdh} = 0.222 \cdot \exp(4.37 \cdot \frac{p}{T} - 1.32 \cdot 10^{-2} \cdot r) \tag{36}$$

At Risø a similar correction for temperature, pressure and humidity is used. Here k is

$$k = k_{ad} \cdot k_{ab} \ , \tag{37}$$

where

$$k_{ad} \simeq k_{pT} \cdot k_{hum} \tag{38}$$

and

$$k_{ab} \simeq k_{sda} \cdot k_{sdh} \tag{39}$$

However, another approximation for the calculation of air density is used. With good approximation k_{ad} for the temperature interval 288.15 K to 298.15 K can be calculated from [13]

$$k_{ad} = \frac{\rho_{ref}}{\rho(p,T,r)} = \frac{T}{2.9053 \cdot p - 0.02563 \cdot r \cdot (\frac{T}{293.15})^{17.97}} \tag{40}$$

The correction k_{ab}, used at Risø for change in air density between source and extrapolation chamber is similar to the correction (Eq. (25)) used at NRC, but here it includes both corrections for changes in pressure, temperature and humidity.

It is assumed that the measured current is directly proportional with the mass of the air volume of the chamber i.e., an increase of the air density of e.g., 3 % will imply a correction factor of 1/1.03 = 0.971. The proportionality between dose rate and air density was confirmed by direct MC calculations performed for a chamber depth of 2000 μm and with a total absorber thickness of 0.95 mg cm^{-2}.

A correction on $\frac{W}{e}$ as a function of humidity has not been done. Instead the value at reference air conditions (note $r_{ref} = 45\,\%$) was associated with an uncertainty [1]:

$$\frac{W}{e} = 33.87 \text{ J C}^{-1} \pm 0.2\,\% \tag{41}$$

3.2 Absorption Coefficient

For low-energy electrons (from e.g., ^{147}Pm) most of the interactions that take place in the entrance window result in a local absorption [2]. The depth dose curve can, as a first approximation, be represented by an exponential function:

$$D(\rho_m \cdot x_m) = D_0 \cdot \exp[-\left(\frac{\mu_{abs}}{\rho}\right)_m \cdot (\rho_m \cdot x_m)] \tag{42}$$

or

$$\ln\left[\frac{D(\rho_m \cdot x_m)}{D_0}\right] = -\left(\frac{\mu_{abs}}{\rho}\right)_m \cdot (\rho_m \cdot x_m)\ , \tag{43}$$

where $(\frac{\mu_{abs}}{\rho})_m$ is the mean mass absorption coefficient in cm^2 mg^{-1} for the β rays, and $(\rho_m \cdot x_m)$ is the penetration depth in mg cm^{-2} of material, m. Eq. (42) may satisfactorily describe depth dose distributions whose shape is not significantly influenced by scatter buildup at shallow depths and/or by degradation of the spectrum at deep layers of the absorber. For ^{147}Pm, a better description can be achieved for $(\rho_m \cdot x_m)$ values up to 10 mg cm^{-2} by introducing the following polynomial function [2]:

$$\ln[D(\rho_m \cdot x_m)] = a_0 + a_1 \cdot (\rho_m \cdot x_m) + a_3 \cdot (\rho_m \cdot x_m)^3\ , \tag{44}$$

where $a_0 = \ln(D_0)$.

By fitting the measured data obtained for the ^{14}C source according to Eqs. (43) and (44) it was found that the correlation coefficient was best for the last fit, and it can be concluded that Eq. (44) represents an adequate expression for the absorption, also for radiation from the ^{14}C source up to a value of $(\rho_m \cdot x_m) = 11$ mg cm^{-2}.

The absorption coefficient of the material m can be derived from

$$\left(\frac{\mu}{\rho}\right)_m = \frac{\mathrm{d}[\ln(D(\rho_m \cdot x_m)/D_0)]}{\mathrm{d}(\rho_m \cdot x_m)} = a_1 + 3 \cdot a_3 \cdot (\rho_m \cdot x_m)^2 \tag{45}$$

The Marquardt-Levenberg algorithm (in SigmaPlot) was used to determine the parameters that minimize the sum of squares of differences between the dependent variable values in the equation models and the observed values. A weighted least square fit was done by using the weighting, w:

$$w = \frac{1}{[\ln(D(\rho_m \cdot x_m))]^2} \tag{46}$$

Depth-dose data were obtained with the extrapolation chamber at NRC using different mylar filters in front of the chamber and using chamber depths ranging from 600 μm to 2400 μm with an interval of 200 μm. The measured dose rates were corrected for pressure and temperature deviation from reference conditions, and the mass absorption coefficients were evaluated for each chamber depth. No influence of chamber depth on the values of a_1 and a_3 was observed in these evaluations, which indicates that depth-dose curves can be satisfactorily obtained

by use of a fixed chamber depth for all absorber thicknesses, and it is therefore not required to obtain a complete extrapolation curve for each absorber thickness. The average values of the coefficients a_1 and a_3 were

$$a_1 = 0.260 \text{ cm}^2 \text{ mg}^{-1} \pm 2.0\,\% \tag{47}$$

and

$$a_3 = 4.3 \cdot 10^{-4} \text{ (cm}^2 \text{ mg}^{-1})^3 \pm 10\,\% \tag{48}$$

For filter thicknesses less than 2.5 mg cm^{-2} the mass absorption coefficient can be described by a_1, though resulting in a maximum deviation of 1 % from the exact calculated value using Eq. (45).

For the ^{14}C source, the absorption coefficients for small thicknesses ($\leq$ 2.5 mg cm^{-2}) of air, graphite, mylar and tissue are listed in Table 1. They have been determined using the calculated absorption coefficient for mylar and the relative attenuation to air, η, for low Z media [12].

$$\left(\frac{\mu_{abs}}{\rho}\right)_m = \eta_m \cdot \left(\frac{\mu}{\rho}\right)_{air} \tag{49}$$

Table 1. Absorption coefficients for small thicknesses ($\leq$ 2.5 mg cm^{-2}) of different media for irradiation with the ^{14}C source.

Medium, m	η_m	$(\frac{\mu_{abs}}{\rho})_m$ [cm^2 mg^{-1}]
Air	1.00	0.252 ± 2.0 %
Graphite	0.96	0.242 ± 2.0 %
Mylar	1.03	0.260 ± 2.0 %
Tissue	1.10	0.278 ± 2.0 %

The absorption coefficient is used for determination of the correction factor k_{ab} (Eqs. (27), (28) and (33) in Sect. 3.1).

3.3 Transmission through Entrance Window

In some situations it may be of interest to know the dose rate, $\dot{D}(0)$, just in front of the entrance window. To be able to estimate $\dot{D}(0)$, a factor, k_{win}, correcting for the absorption and scattering caused by the window material, is employed. The value of this correction factor for a certain β source depends on the degradation of the β spectrum, and it must be evaluated for each irradiation configuration separately.

The entrance window of the extrapolation chamber used at NRC consists of a 3.4 μm mylar foil coated with a graphite layer for electrical conductivity. The total thickness is (0.954 ± 0.095) mgcm^{-2}. The correction factor k_{win}, the ratio between the dose to the air cavity without and with the entrance window, was calculated using correlated sampling and was evaluated from the fit for the measured data as well. The calculations were performed for chamber depths ranging from 800 to 2400 μm with no filters but the entrance window. The MC calculated average value of k_{win} for all chamber depths, assuming no uncertainty in the window thickness, was

$$k_{win,calc} = 1.211 \pm 0.5\,\% \tag{50}$$

The graphite layer has a thickness equivalent to 0.446 mg cm^{-2} of mylar. The total thickness of the entrance window was then 0.922 mg cm^{-2} of mylar with an

uncertainty on the thickness of 10%. The result of the measurement was calculated from Eq. (44) according to

$$k_{win,NRC} = \exp[a_{1,mylar} \cdot (\rho \cdot x)_{mylar} + a_{3,mylar} \cdot (\rho \cdot x)_{mylar}{}^3] = 1.27 \pm 2.6\,\% \quad (51)$$

The measured and calculated values of k_{win} agree reasonably well. For comparison, the value of k_{win} for ^{147}Pm for a distance of 20 cm and with beam flattening filter is 1.201 ± 2.0 % [11].

At Risø the window thickness is 0.66 mg cm^{-2} of graphite coated mylar. Using Eq. (44), this results in a transmission through entrance window of

$$k_{win,Risø} = 1.19 \pm 1.7\,\% \quad (52)$$

3.4 Backscatter

The difference in backscattering between tissue and collector electrode material (PMMA and graphite layer) has been calculated using correlated sampling. The backscatter from the PMMA with the graphite layer (collector electrode) results in a dose to the air, which was 0.987 ± 0.4 % times the dose in the case of using tissue as backwall material (without a graphite layer). To convert the measured dose to a dose in an extrapolation chamber model of tissue, it must be multiplied by a factor k_{bak} = 1.013 ± 0.4 %. Normally it is assumed that the difference in backscattering properties is negligible for very low energy β particles from ^{147}Pm. For ^{204}Tl and ^{90}Sr/^{90}Y the backscatter correction factor is 1.010 [1, 11].

3.5 Sidewall Effect

MC calculations using correlated sampling and with sidewalls of PMMA in one case and of air in another, were performed to find the effect of the sidewalls. As could be expected from considering the energy of the electrons and the distance between collecting volume and the sidewalls, there is no effect. The results for different chamber depths and filter thicknesses was k_{sw} = 1.0003 ± 0.08 % (ratio of dose in case with air walls to dose in case of walls of PMMA).

3.6 Stopping Power Ratio, Tissue to Air

Two methods of calculating the stopping power ratio, tissue to air, has been used. One method is to calculate the stopping power ratio for the average energy of the spectrum in the collector volume behind the entrance window. Collision stopping powers for different media show similar trends as a function of particle energy, thus the ratio for two media is a very slowly varying function [15]. This means that the stopping power ratio is reasonably well approximated through simple estimation by calculating, using tabulated values, the stopping powers for the actual media at the average energy of electrons crossing the cavity.

Mass collision stopping power ratios, tissue to air, for a range of electron energies was calculated using the method described by Seltzer and Berger [16]. The uncertainty on the calculated stopping power ratio was estimated to 1 – 2 %. The air was dry air near sea level and the tissue is the ICRU four-component soft tissue. The composition of this tissue related to mass is 76.18 % O, 10.12 % H, 11.1 % C and 2.60 % N. Its density is 1.000 g cm^{-3}. In Table 2, the calculated stopping power ratios, tissue to air, $s_{t,a}$, are shown for different energies.

The MC calculated average energy of the electron spectrum at a distance of 50 mm in air was 55 keV [3]. At this energy the mass collision stopping power ratio,

tissue to air, is

$$s_{t,a} = 1.124 \pm 2\,\% \tag{53}$$

Table 2. Mass collision stopping power ratios, tissue to air, $s_{t,a}$, for electrons of different energies.

Energy [keV]	$s_{t,a}$
60	1.124 ± 2 %
50	1.124 ± 2 %
40	1.125 ± 2 %
30	1.126 ± 2 %
20	1.128 ± 2 %
10	1.132 ± 2 %
5	1.137 ± 4.2 %
2	1.146 ± 10 %

Another method is MC calculation. Using the EGS4 code SPRRZ the stopping power ratio, tissue to air, in the collector volume in the extrapolation chamber was calculated using the simplified source model. The SPRRZ code uses unrestricted stopping powers for computation. The tissue material was also ICRU four-component soft tissue. The ratio was calculated for chamber depths ranging from 400 to 2400 μm with intervals of 400 μm and with different filters (0 – 10.82 mgcm^{-2} tissue equivalent) in front of the window resulting in energy in the chamber varying from 50 keV and down to a few keV. The electron cutoff energy was 521 keV. The average value of the MC calculated stopping power ratio was

$$s_{t,a} = 1.133 \pm 0.7\,\% \tag{54}$$

The uncertainty of 0.7 % on $s_{t,a}$ is a minimum value due to uncertainties in the stopping powers [17].

4 Measured and Calculated Dose Rates

In this chapter results from measurements by extrapolation chamber of absorbed dose rate to tissue at different tissue depths are compared with data obtained from MC calculations.

4.1 Dose Rates in Collector Volume in Extrapolation Chamber

In Sect. 2.2, the calculated dose rate to the air cavity, c, in the extrapolation chamber was found to be calculated from

$$\dot{D}_{c,cal}(d) = (1.31 \cdot 10^6 \pm 2.5\,\%) \cdot D'_e(d) + (3.31 \cdot 10^4 \pm 3.4\,\%) \cdot D'_{ph}(d) \qquad (55)$$

However, the dose contribution from photons is only about 0.02 % for low filter thicknesses (increasing to about 1 % of the total dose at a tissue depth of 10 $\mathrm{mg\,cm^{-2}}$) and can be considered insignificant compared to the dose from electrons. The calculated dose rate in air can then be calculated from

$$\dot{D}_{c,cal}(d) \simeq (1.31 \cdot 10^6 \pm 2.5\,\%) \cdot D'_e(d) \qquad (56)$$

The measured dose rate is obtained from Eq. (16) with $\frac{W}{e} = 33.87 \pm 0.2\,\%$ and $\rho_{ref} = 1.1995\ \mathrm{kg\,m^{-3}}$. For the extrapolation chamber at NRC, having an effective collector area of $7.093 \cdot 10^{-4}$ $\mathrm{m^2}$ $\pm$ 0.07 %, the measured dose rate in $\mu\mathrm{Gy\,s^{-1}}$, at reference air conditions, is

$$\begin{aligned}\dot{D}_{c,NRC}(d) &= \frac{33.87 \pm 0.1\,\%}{(7.093 \cdot 10^{-4} \pm 0.07\,\%) \cdot 1.1995} \cdot \left(\frac{\mathrm{d}(I_{cor})}{\mathrm{d}l}\right)_{l\to 0} \\ &= (39.81 \pm 0.1\,\%) \cdot \left(\frac{\mathrm{d}(I_{cor})}{\mathrm{d}l}\right)_{l\to 0}\ , \end{aligned} \qquad (57)$$

where $\left(\frac{\mathrm{d}(I_{cor})}{\mathrm{d}l}\right)_{l\to 0}$ is measured in $\mathrm{fA\,\mu m^{-1}}$. Similarly, the measured dose rate for the extrapolation chamber at Risø, having an effective collector area of $7.16 \cdot 10^{-4}$ $\mathrm{m^2}$ $\pm$ 0.3 %, is

$$\begin{aligned}\dot{D}_{c,Risø}(d) &= \frac{33.87 \pm 0.1\,\%}{(7.16 \cdot 10^{-4} \pm 0.3\,\%) \cdot 1.1995} \cdot \left(\frac{\mathrm{d}(I_{cor})}{\mathrm{d}l}\right)_{l\to 0} \\ &= (39.4 \pm 0.3\,\%) \cdot \left(\frac{\mathrm{d}(I_{cor})}{\mathrm{d}l}\right)_{l\to 0} \end{aligned} \qquad (58)$$

In Table 3, the dose rates in the air cavity of the extrapolation chamber, obtained from MC calculation and from measurements with no absorber in front of the entrance window, is shown. The dose rate measured at NRC has a high uncertainty, which makes the dose rate agree with both the MC calculated dose rate and the dose rate measured at Risø. Comparing the MC calculated dose rate with the one measured at Risø shows a difference of

$$\frac{\dot{D}_{c,Risø}(d_w)}{\dot{D}_{c,cal}(d_w)} = 1.07 \pm 3.6\,\% \qquad (59)$$

In Figs. 6 and 7, the depth - dose-rate profiles measured at NRC and Risø, respectively, are compared with the results of the MC simulations of the extrapolation chamber measurements. The nominal values of the dose rates are tabulated in App. B.1. The results obtained at the two laboratories agreed very well within the uncertainty limits. The measured dose rates were about 10 % higher than

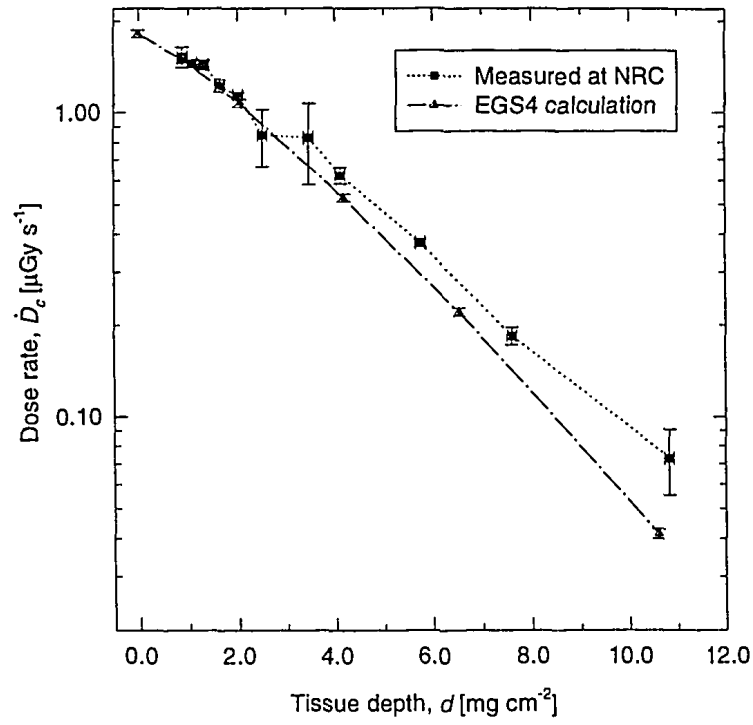

Figure 6. Dose rate in air in the extrapolation chamber collector volume at 50 mm distance from the ^{14}C source. The dose rates measured at NRC are compared with the values calculated using EGS4.

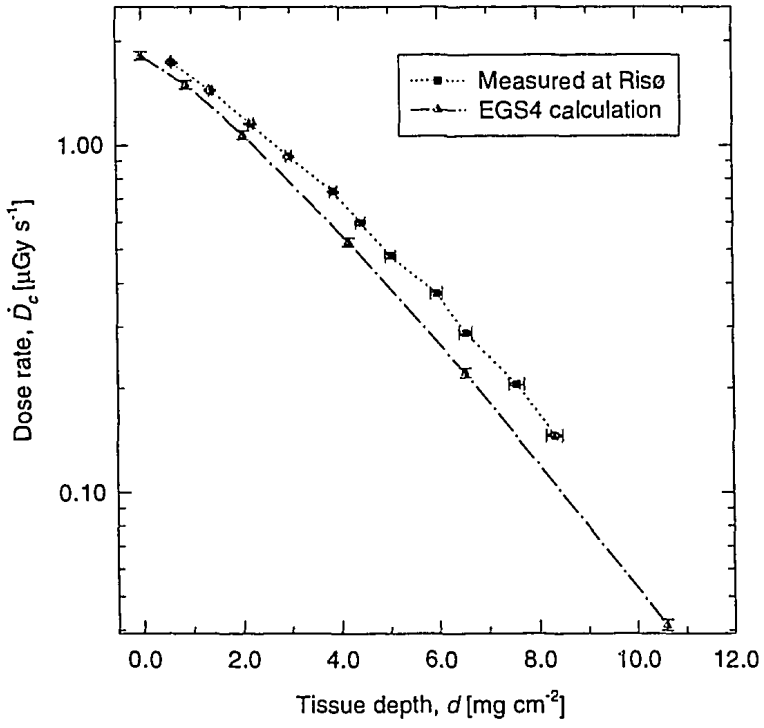

Figure 7. Dose rate in air in the extrapolation chamber collector volume at 50 mm distance from the ^{14}C source. The dose rates measured at Risø are compared with the values calculated using EGS4.

Table 3. Dose rates in the air cavity of the extrapolation chamber obtained from MC calculation and from measurements with no absorber in front of the entrance window. The dose rate given for the extrapolation chamber measurement at Risø is transformed to a window thickness equal to the one for the NRC extrapolation chamber for comparison.

Dose rate	$d_w = 0.954$ mg cm^{-2}
$\dot{D}_{c,cal}(d_w)$	1.50 ± 3%
$\dot{D}_{c,NRC}(d_w)$	1.53 ± 9%
$\dot{D}_{c,Risø}(d_w)$	1.61 ± 2%

the MC calculated dose rates for experiments with absorber thicknesses below 1 mg cm^{-2}. However, the difference between measured and calculated dose rates increased to about 40 % for a total absorber thickness of 8 mg cm^{-2}, which is seen in Fig. 8.

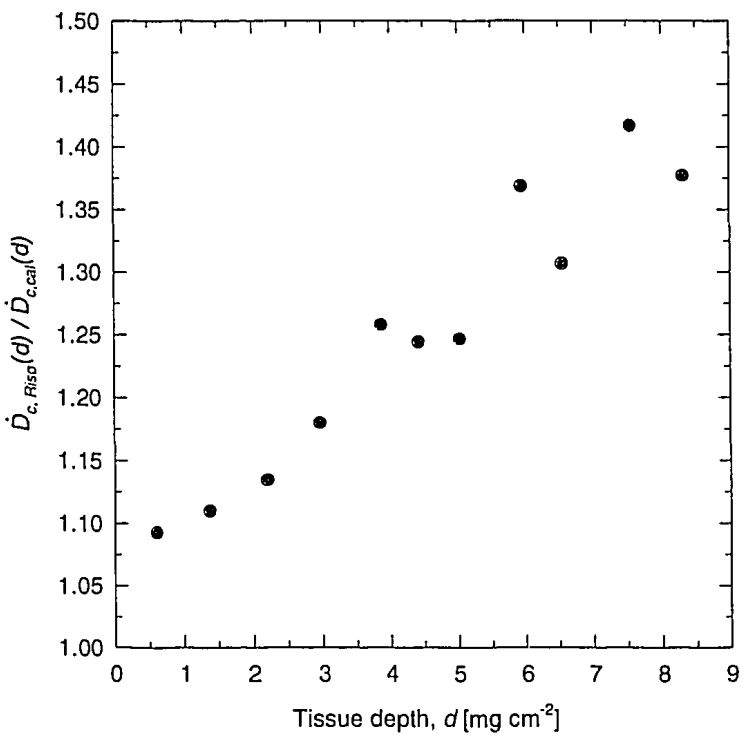

Figure 8. Relative difference in dose rate in air in the extrapolation chamber collector volume at 50 mm distance from the ^{14}C source.

Comparing the shapes of the measured and the calculated depth - dose-rate in air profiles, the calculated curve decreases faster than the measured. An explanation for this may be that the EGS4 code is not usable for simulating transport of electrons with very low energies. From the particle pulse height distribution for the particles in the collector air volume in the MC calculation with 7 mg cm^{-2}, it was found that about 45 % of the electrons had an energy below 10 keV, whereas for no window or absorber only 2 – 3 % of the electrons had an energy below 10 keV.

A reason for the difference between measured and calculated dose rates, even at low tissue depths, may be that the dose rate to air evaluated from MC calcu-

lations were performed for a model of the extrapolation chamber with a chamber depth, l, of 2000 μm and resulting in an average dose to this air volume. In the measurements the dose rates were obtained by extrapolating to $l = 0$ i.e., just behind the entrance window. This means that the dose to the air in the collector volume will be smaller for $l = 2000$ μm than for smaller chamber depths, due to the attenuation in the air volume. For comparison the dose rates measured with a fixed chamber depth of 400 μm is 10 % higher than the dose rates measured with a fixed depth of 2000 μm. However, the extrapolated values of the measured dose rates were only 5 % higher than the measured dose rates at 2000 μm chamber depth. The shape of the depth-dose curve was the same for all depths ranging from 600 to 2400 μm. Performing MC calculations with a scoring volume just behind the entrance window and only 100 μm thick is expected to result in better agreement between measured and calculated values of the dose rates to air for small absorber thicknesses ($d < 1$ mg cm^{-2}).

Another reason for the deviation between measured and calculated dose rates may be an uncertainty on the source strength, which is not stated by the manufacturer.

4.2 Dose Rates in Tissue

To obtain the dose in tissue instead of air, the dose in air must be multiplied by the stopping power ratio, tissue to air, $s_{t,a}$, and the factor, k_{bak}, correcting for the difference in backscatter between tissue and PMMA. $s_{t,a}$ has been calculated earlier to be 1.133 ± 0.7 % (Sect. 3.6), and k_{bak} was calculated to 1.013 ± 0.4 % (Sect. 3.4).

The calculated dose rate in tissue is then

$$\dot{D}_{t,cal}(d) = s_{t,a} \cdot k_{bak} \cdot \dot{D}_{c,cal}(d) = (1.504 \cdot 10^6 \pm 2.6\,\%) \cdot D'_c(d) \qquad (60)$$

Similarly, the measured dose rates in tissue were calculated from

$$\dot{D}_{t,NRC}(d) = s_{t,a} \cdot k_{bak} \cdot \dot{D}_{c,NRC}(d) = (45.7 \pm 0.8\,\%) \cdot \left(\frac{\mathrm{d}(I_{cor})}{\mathrm{d}l}\right)_{l \to 0} \qquad (61)$$

and

$$\dot{D}_{t,Riso}(d) = s_{t,a} \cdot k_{bak} \cdot \dot{D}_{c,Riso}(d) = (45.3 \pm 0.9\,\%) \cdot \left(\frac{\mathrm{d}(I_{cor})}{\mathrm{d}l}\right)_{l \to 0} \qquad (62)$$

The measured dose rates in tissue are tabulated in App. B.2.

To test the validity of the extrapolation chamber MC model for calculation of absorbed dose rate in tissue, MC calculations were also performed using a complete tissue phantom. The dose to tissue in a geometry similar to that of the extrapolation chamber was calculated using the EGS4 code DOSRZ. The distance from source to surface of tissue was 50 mm, the radius of the tissue cylinder was 100 mm and the height of this cylinder was 60 mm - based on a complete absorption of 20 keV bremsstrahlung photons. It was divided into radii of 15 mm (the radius of the collector electrode), 25 mm and 40 mm and into slabs of equal thicknesses of $1.0 \cdot 10^{-2}$ mm (= 1 mg cm^{-2}). The dose in each slab was calculated as a function of slab number and radius.

The dose from the electron spectrum was calculated as well as from the photon spectrum (bremsstrahlung from the source). The total dose was calculated using the ratio of fluences at 50 mm distance for complete to simplified model of source (Eq. (4)). In App. B.2, the MC calculated dose rates in tissue (the scoring region has an outer radius of 15 mm) are tabulated. In Fig. 9, the calculated dose rates in tissue are shown for scoring regions between different radii. The dose rate decreases as the radius of the scoring region is increased, which is due to the inhomogeneity

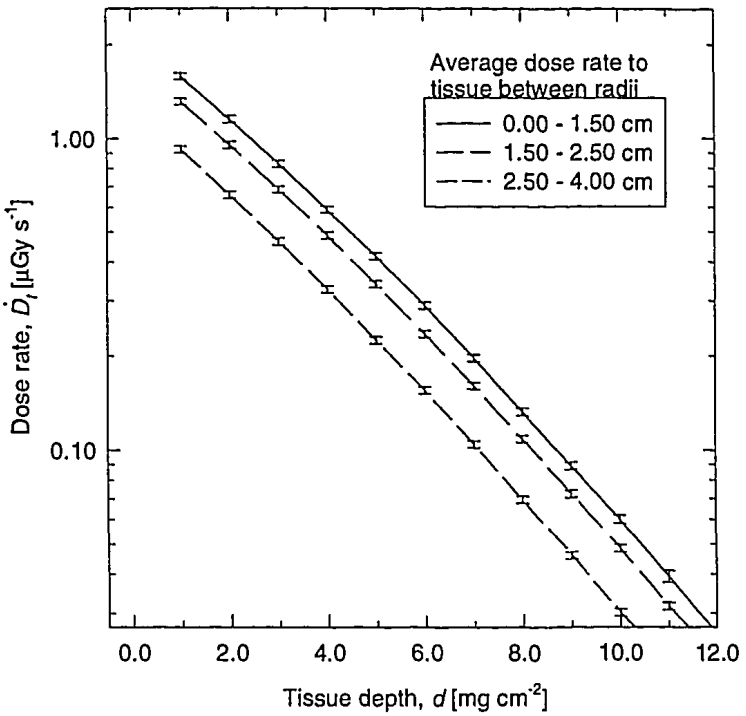

Figure 9. Calculated dose rate to tissue at 50 mm distance in air from the ^{14}C source for different radii of scoring regions of the tissue phantom and for different tissue depths.

of the radiation field. The dose contribution from photons amounts to less than 1 % of the dose from electrons for all data shown in the figure.

The calculated dose rates in tissue, using the extrapolation chamber model, were all higher than the dose rates calculated for the tissue cylinder (Fig. 10). In Fig. 11, the ratio of the dose rate calculated from simulating the extrapolation chamber measurement, $\dot{D}_{t,ext.ch.}$, to the dose rate calculated for the tissue phantom with 15 mm radius, $\dot{D}_{t,tis.cyl.}$, is shown. There appeared to be a dose buildup in the simulation of the extrapolation chamber measurement, which was not seen for simulations with the tissue cylinder. The reason for this dose buildup should be studied further, and corrected for when performing extrapolation chamber measurements.

4.3 Transmission Factor

In dosimetry of weakly penetrating radiation, the dose in tissue at a depth of 7 mg cm^{-2} is of particular interest. The transmission factor, $T(7\ \text{mg cm}^{-2})$, is the ratio of dose at 7 mg cm^{-2} depth to dose at 0 mg cm^{-2} (the surface of the entrance window). 7 mg cm^{-2} tissue is equivalent to 7.48 mg cm^{-2} mylar using the relative attenuation factors in Sect. 3.2. The uncertainty on the total absorber thickness was assumed to be 0.2 mg cm^{-2}. Using Eq. (44), $T(7\ \text{mg cm}^{-2})$ was calculated to

$$T_{NRC}(7\ \text{mg cm}^{-2}) = \frac{D(7\ \text{mg cm}^{-2})}{D(0\ \text{mg cm}^{-2})}$$
$$= \exp[a_1 \cdot 7.48\ \text{mg cm}^{-2} + a_3 \cdot (7.48\ \text{mg cm}^{-2})^3] = 0.119 \pm 7\ \% \qquad (63)$$

From the MC calculations using the extrapolation chamber model and the tissue phantom, the transmission factor was also found by fitting $\ln(D)$ to

$$\ln[D(\rho_m \cdot x_m)] = a_0 + a_1 \cdot (\rho_m \cdot x_m) + a_3 \cdot (\rho_m \cdot x_m)^3\ , \qquad (64)$$

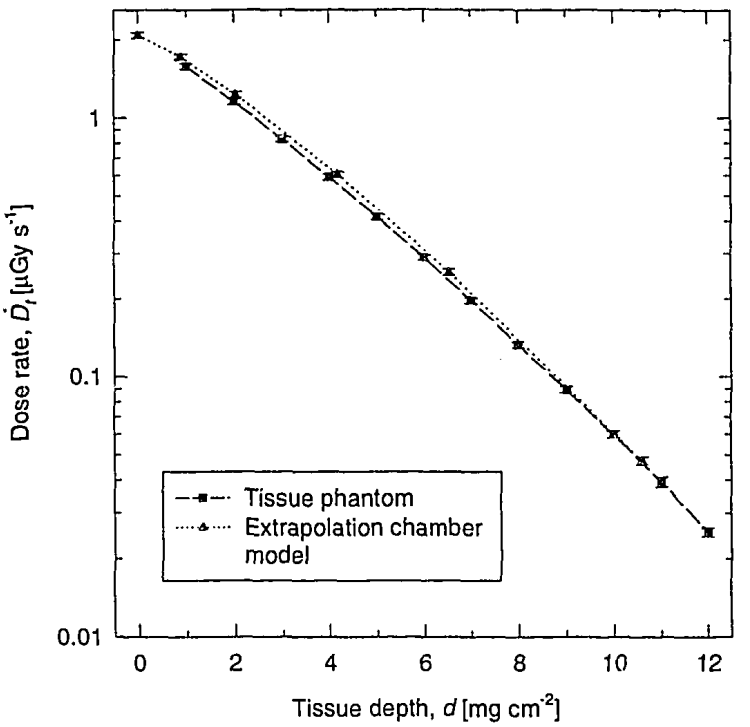

Figure 10. MC calculated dose rates in tissue from simulations of the tissue phantom and the extrapolation chamber measurements.

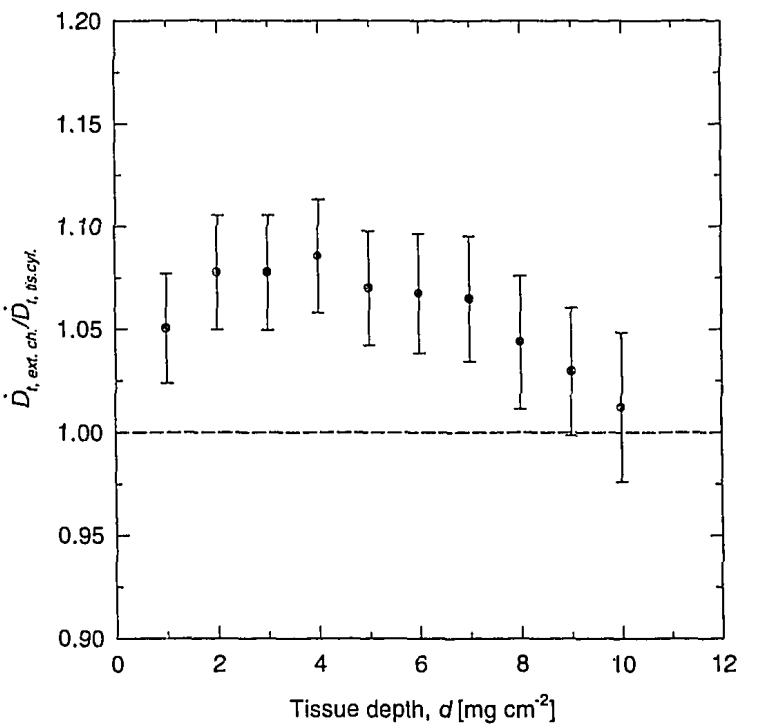

Figure 11. Ratios of calculated dose rates in tissue at 50 mm distance from the ^{14}C source. The dose rates were calculated for a cylindrical tissue phantom and by simulating the extrapolation chamber measurement having a chamber depth of 2000 µm.

where $a_0 = \ln(D_0)$. The assumed uncertainty on the total absorber thickness was 0.2 mg cm^{-2}.

$$T_{ext.ch.}(7 \text{ mg cm}^{-2}) = 0.109 \pm 8\,\% \tag{65}$$

$$T_{tissue}(7 \text{ mg cm}^{-2}) = 0.091 \tag{66}$$

The transmission factor for the measurement at NRC and for the MC calculation with the extrapolation chamber model agrees well.

5 Conclusions

The extrapolation chamber measurement technique and the Monte Carlo calculation technique based on the EGS4 system have been studied for application for determination of dose rates in a low-energy β radiation field e.g., that from the ^{14}C source.

Various details of the extrapolation chamber measurement method and evaluation procedure have been studied and further developed, and a complete procedure for the experimental determination of dose rates from a ^{14}C source have been presented. A number of correction factors and other parameters, used in the evaluation procedure for the measured data, have been obtained by MC calculations. It can be concluded that the MC calculation technique is a valuable tool in the development of a complete extrapolation chamber measurement method. The theoretical correction for change in air density from reference density was confirmed by MC calculations. Parameters, which have been achieved by MC calculations, include factors correcting for transmission through entrance window, k_{win}, backscatter difference, k_{bak}, and sidewall effect, k_{sw}. An interesting result was obtained from the calculation of k_{bak}, showing a value of 1.013. Correction for backscatter difference is usually considered negligible for low-energy β radiation. Also the stopping power ratio, tissue to air, $s_{t,a}$, have been calculated by the EGS4 code and compared with data obtained by the method described by Seltzer and Berger [16]. The stopping power ratios obtained by the two methods showed fine agreement.

The dose rate at 50 mm from the ^{14}C source was measured with extrapolation chambers at two laboratories, NRC and Risø, respectively. The results obtained at the two laboratories agreed very well within the uncertainty limits. It was confirmed by measurements of dose rates using different absorbers in front of the extrapolation chamber that the fitting procedure previously reported for depth-dose profiles for β radiation from ^{147}Pm [2] is suitable, also for β radiation from a ^{14}C source.

The EGS4 system was used for a complete modelling of the extrapolation chamber measurement method, as well as for direct determination of depth-dose data using a cylindrical model consisting of tissue. The results of calculations with the extrapolation chamber model showed an increasing difference compared with the measurements for increasing absorber thicknesses. For absorber thicknesses below 1 mg cm^{-2}, the measured dose rates were about 10 % higher than the calculated dose rates, and at 7 mg cm^{-2} the difference was 35 %. An explanation for this may be that the EGS4 code is not usable for simulating transport of electrons with very low energies. From the particle pulse height distribution in the MC calculation with 7 mg cm^{-2}, it was found that about 45 % of the electrons had an energy below 10 keV, whereas for no window or absorber, only 2 – 3 % of the electrons had an energy below 10 keV.

Even at low tissue depths there is a difference between measured and calculated dose rates, which can be explained by the calculated dose being an average dose in the collector volume with $l = 2000\,\mu$m, whereas the measured dose rate is found by extrapolating to $l = 0\,\mu$m.

MC simulations with the tissue phantom showed a dose buildup compared with the simulation of the extrapolation chamber measurement. The reason for this dose buildup should be studied further, and corrected for when performing extrapolation chamber measurements.

To obtain the dose behind the entrance window at 2000 μm chamber depth with an uncertainty of 0.3 %, the calculation time was 50 hours ($55 \cdot 10^6$ histories) on the NRC SGI R4400 computers.

5.1 Suggestions for Further Studies

The data measured with the extrapolation chamber are fitted to a second order polynomium. In this fitting procedure, the weighting should be studied further. Putting too much weight on small chamber depths may result in too high a value of the estimated dose rate.

MC calculation of the dose in a very thin air volume, just behind the entrance window, would clarify whether the higher doses obtained by extrapolation chamber measurements are due to attenuation in the air volume, or they can be explained by the uncertainty on the source strength.

A dose buildup appeared in the simulation of the extrapolation chamber measurement, which was not seen for simulations with the tissue cylinder. The reason for this dose buildup should be studied further.

Acknowledgements

I would like to thank Dave Rogers for making it possible for me to spend 6 months in the group Ionizing Radiation Standards (IRS), NRC, Canada, where calculations and part of the experiments, described in this report, were performed. Also thanks to Dave Rogers and Len van der Zwan, IRS, for their indispensable guidance and help during my studies there. And not least, the rest of the group, Ionizing Radiation Standards, are to be thanked for each of them being of great inspiration both professionally and socially.

And finally, thanks to my advisor at Risø, Poul Christensen, for guidance during the writing of this report.

References

[1] Böhm, J.: PTB-Dos-13, The National Primary Standard of the PTB for Realizing the Unit of the Absorbed Dose Rate to Tissue for Beta Radiation, April 1986.

[2] Francis, T. M., Böhm, J., Chartier, J.-L., Christensen, P.: Experience gained on Extrapolation Chamber Measurement Techniques from an Intercomparison Exercise conducted with a ^{147}Pm Source, Rad. Prot. Dos., Vol. 39, No. 1/3 pp. 109-114, 1991.

[3] Borg, J.: Monte Carlo Calculations and Measurements of Spectra from a C-14 Source, Risø–R–893(EN), May 1996.

[4] Nelson, W. R., Hirayama, H., Rogers, D. W. O.: The EGS4 Code System, SLAC-Report-265, Dec. 1985.

[5] Amersham: Product specification, Data sheet 11954D, Aug. 1989.

[6] Bielajew, A. F., Rogers, D. W. O.: PRESTA: The Parameter Reduced Electron-Step Transport Algorithm for Electron Monte Carlo Transport, Nuclear Instruments and Methods B18, pp. 165-181, 1987.

[7] Malamut, C, Rogers, D. W. O., Bielajew, A. F.: Calculation of Water/Air Stopping-Power Ratios using EGS4 with Explicit Treatment of Electron - Positron Differences, Med. Phys., Vol. 18, pp. 1222-1228, 1991.

[8] Rogers, D. W. O., Bielajew, A. F.: Monte Carlo Techniques of Electron and Photon Transport for Radiation Dosimetry, in "The Dosimetry of Ionizing Radiation", Vol. III, eds. K. R. Kase, B. E. Bjarngard, and F. H. Attix, (Academic Press), pp. 427-539, 1990.

[9] Kosunen, A., Rogers, D. W. O.: Beam Quality Specification for Photon Beam Dosimetry, Med. Phys., Vol. 20, pp. 1181-1188, 1993.

[10] Ma, C., Nahum, A. E.: Calculation of Absorbed Dose Ratios using Correlated Monte Carlo Sampling, Med. Phys. 20 (4), pp. 1189-1199, 1993.

[11] van der Zwan, L., Geiger, K. W.: The β-Calibration Facility at the National Research Council of Canada, Report PIRS-0093, 1986.

[12] Cross, W. G., Ing, H., Freedman, N. O., Mainville, J.: Tables of Beta-ray Dose Distributions in Water, Air and other Media, AECL-7617, Sept. 1982.

[13] Drake, K.-H., Böhm, J.: PTB-Dos-19, Automatisierter Meßstand für die Dosimetrie von Betastrahlung, April 1990.

[14] Giacomo, P.: Equation for the Determination of the Density of Moist Air, Metrologia 18, pp. 33-40, 1982.

[15] Attix, F. H.: Introduction to Radiological Physics and Dosimetry, 1986.

[16] Seltzer, S. M., Berger, M. J.: Evaluation of the Collision Stopping Power of Elements and Compounds for Electrons and Positrons, Int. J. Appl. Radiot. Isot., Vol. 33, pp. 1189-1218, 1982.

[17] Rogers, D. W. O.: private communication.

[18] Chartier, J.-L.: Proposal for a Simplified Procedure to Evaluate the Uncertainties in Extrapolation Chamber Measurements, Eurados WG N° 2, 1994.

A Measurement Uncertainties

The uncertainty on the measurements with extrapolation chambers consists of type A and type B uncertainties. Type A uncertainties (s_i) are evaluated by statistical methods, and type B uncertainties (u_i) are evaluated by approximations to the variances (u_i^2) corresponding to known or assumed values [18].

The estimation $s^2(x)$ of the variance of any single random measurement x made by a radiation detector should be determined from the data of n such measurements by means of the equation [15]:

$$s^2(x) = \frac{1}{n-1}\sum_{i=1}^{n}(x_i - \overline{x})^2 \ , \tag{A.1}$$

where

$$\overline{x} = \frac{1}{n}\sum_{i=1}^{n} x_i \tag{A.2}$$

The estimated variance of the mean value $\overline{x}$ (or square of standard error) is obtained from experimental data by

$$s^2(\overline{x}) = s^2(x)/n \tag{A.3}$$

Type B uncertainties (u_i) are considered as approximations to the corresponding variances, which are assumed existing. The quantities u_i^2 are treated like variances and the quantities u_i like standard deviations.

The combined uncertainty or standard deviation on the value $y = F(x_1, x_2, ...)$ being a function of uncorrelated variables, x_i, with respective standard deviations s_i and u_i, is obtained approximately by

$$S_y = \sqrt{\sum_i (\frac{\partial F}{\partial x_i})^2 (s_i^2 + u_i^2)} \tag{A.4}$$

The values of the type B uncertainties are listed in Table 4.

Table 4. Values and uncertainties of main parameters and correction factors used for the determination of the dose rates in tissue equivalent material by use of the extrapolation chamber.

Parameter	Value	Relative standard deviation in %
W/e	33.87 J C^{-1}	0.1
$s_{t,a}$	1.128	0.02
a (NRC)	7.093 cm^2	0.07
a (Risø)	7.16 cm^2	0.3
ρ_{ref}	1.200 kg m^{-3}	0.04
k_{bak}	1.013	0.4
k_{sw}	1.0003	0.08
k_{dc}	1	0
k_{ad}	-	-
k_{ab}	-	-
k_{win} (NRC)	1.27	2.6
k_{win} (Risø)	1.19	1.7

B Dose Rates in Air and Tissue

B.1 Dose Rates in Air

The dose rates in air was calculated by MC simulations of the extrapolation chamber measurements, and measured with the extrapolation chambers set up at NRC and at Risø. In Tables 5 to 7, the dose rates in air are listed. The absorber thickness is given in tissue equivalent thickness.

Table 5. MC calculated dose rates in air i.e., the collector volume of the extrapolation chamber.

Tissue depth, d [mg cm^{-2}]	Dose rate, $\dot{D}_c$ [μGy s^{-1}]	$\sigma_{rel}(\dot{D}_c)$ [%]
0.000	1.815	2.8
0.887	1.498	2.8
2.038	1.073	2.9
4.179	0.527	2.8
6.536	0.222	3.0
10.59	0.0414	3.6

Table 6. Dose rates in air measured with the extrapolation chamber at NRC.

Tissue depth, d [mg cm^{-2}]	Dose rate, $\dot{D}_c$ [μGy s^{-1}]	$\sigma_{rel}(\dot{D}_c)$ [%]
0.88	1.528	7.7
1.08	1.455	2.8
1.31	1.434	3.6
1.64	1.225	4.6
2.01	1.137	2.5
2.52	0.843	21
3.46	0.828	30
4.12	0.624	6.0
5.76	0.375	2.8
7.60	0.185	6.7
10.83	0.073	24

Table 7. Dose rates in air measured with the extrapolation chamber at Risø.

Tissue depth, d [mg cm^{-2}]	Dose rate, $\dot{D}_c$ [μGy s^{-1}]	$\sigma_{rel}(\dot{D}_c)$ [%]
0.61	1.737	0.5
1.38	1.441	0.6
2.20	1.153	0.6
2.97	0.928	0.7
3.87	0.734	0.6
4.42	0.600	0.9
5.03	0.480	0.8
5.96	0.375	0.8
6.55	0.288	1.3
7.56	0.206	1.0
8.32	0.146	0.9

B.2 Dose Rates in Tissue

The dose rates in tissue was calculated by MC simulating the absorbed dose in a tissue cylinder, and measured with the extrapolation chambers set up at NRC and at Risø, applying the correction factors and the stopping power ratio, tissue to air. In Tables 8 to 10, the dose rates in tissue are listed. The absorber thickness is given in tissue equivalent thickness.

Table 8. MC calculated dose rates in tissue for a scoring region with radius 15 mm.

Tissue depth, d [mg cm^{-2}]	Dose rate, $\dot{D}_t$ [μGy s^{-1}]	$\sigma_{rel}(\dot{D}_t)$ [%]
1.00	1.584	2.5
2.00	1.155	2.5
3.00	0.830	2.5
4.00	0.591	2.5
5.00	0.418	2.5
6.00	0.290	2.6
7.00	0.197	2.7
8.00	0.133	2.7
9.00	0.089	2.8
10.00	0.060	3.1
11.00	0.039	4.3
12.00	0.025	3.9

Table 9. Dose rates in tissue measured with the extrapolation chamber at NRC.

Tissue depth, d [mg cm^{-2}]	Dose rate, $\dot{D}_t$ [μGy s^{-1}]	$\sigma_{rel}(\dot{D}_t)$ [%]
0.88	1.753	7.7
1.08	1.670	2.9
1.31	1.645	3.6
1.64	1.406	4.7
2.01	1.305	2.5
2.52	0.968	21
3.46	0.950	30
4.12	0.716	6.0
5.76	0.430	2.9
7.60	0.212	6.7
10.83	0.084	24

Table 10. Dose rates in tissue measured with the extrapolation chamber at Risø.

Tissue depth, d [mg cm^{-2}]	Dose rate, $\dot{D}_t$ [μGy s^{-1}]	$\sigma_{rel}(\dot{D}_t)$ [%]
0.61	1.994	0.9
1.38	1.653	1.0
2.20	1.323	1.0
2.97	1.066	1.1
3.87	0.842	1.0
4.42	0.688	1.2
5.03	0.551	1.1
5.96	0.430	1.2
6.55	0.331	1.5
7.56	0.236	1.3
8.32	0.168	1.2

Bibliographic Data Sheet **Risø–R–894(EN)**

Title and author(s)

Dose Rates from a C-14 Source using Extrapolation Chamber and MC Calculations

Jette Borg

ISBN	ISSN
87–550–2180–8	0106–2840

Dept. or group	Date
Department of Nuclear Safety Research and Nuclear Facilities	May 1996

Groups own reg. number(s)	Project/contract No.

Pages	Tables	Illustrations	References
35	10	11	18

Abstract (Max. 2000 char.)

The extrapolation chamber technique and the Monte Carlo (MC) calculation technique based on the EGS4 system have been studied for application for determination of dose rates in a low-energy β radiation field e.g., that from a ^{14}C source. The extrapolation chamber measurement method is the basic method for determination of dose rates in β radiation fields. Applying a number of correction factors and the stopping power ratio, tissue to air, the measured dose rate in an air volume surrounded by tissue equivalent material is converted into dose to tissue. Various details of the extrapolation chamber measurement method and evaluation procedure have been studied and further developed, and a complete procedure for the experimental determination of dose rates from a ^{14}C source is presented. A number of correction factors and other parameters used in the evaluation procedure for the measured data have been obtained by MC calculations.

The whole extrapolation chamber measurement procedure was simulated using the MC method. The measured dose rates showed an increasing deviation from the MC calculated dose rates as the absorber thickness increased. This indicates that the EGS4 code may have some limitations for transport of very low-energy electrons i.e., electrons with estimated energies less than $10 - 20$ keV.

MC calculations of dose to tissue were performed using two models: a cylindrical tissue phantom and a computer model of the extrapolation chamber. The dose to tissue in the extrapolation chamber model showed an additional buildup dose compared to the dose in the tissue model.

Descriptors INIS/EDB

BETA DOSIMETRY; BETA SOURCES; CARBON 14; COMPUTERIZED SIMULATION; DOSE RATES; E CODES; EXPERIMENTAL DATA; EXTRAPOLATION CHAMBERS; MONTE CARLO METHOD; STOPPING POWER; TISSUE-EQUIVALENT MATERIALS

Available on request from:
Information Service Department, Risø National Laboratory
(Afdelingen for Informationsservice, Forskningscenter Risø)
P.O. Box 49, DK–4000 Roskilde, Denmark
Phone (+45) 46 77 46 77, ext. 4004/4005 · Fax (+45) 46 75 56 27 · Telex 43 116

RISØ

Objective

Risø's objective is to provide society and industry with new opportunities for development in three main areas:

- *Energy technology and energy planning*
- *Environmental aspects of energy, industrial and agricultural production*
- *Materials and measuring techniques for industry*

In addition, Risø advises the authorities on nuclear issues.

Research profile

Risø's research is strategic, which means that it is long-term and directed toward areas which technological solutions are called for, whether in Denmark or globally. The reasearch takes place within 11 programme areas:

- *Wind energy*
- *Energy materials and energy technologies for the future*
- *Energy planning*
- *Environmental impact of atmospheric processes*
- *Processes and cycling of matter in ecosystems*
- *Industrial safety*
- *Environmental aspects of agricultural production*
- *Nuclear safety and radiation protection*
- *Structural materials*
- *Materials with special physical and chemical properties*
- *Optical measurement techniques and information processing*

Transfer of Knowledge

Risø's research results are transferred to industry and authorities through:

- *Co-operation on research*
- *Co-operation in R&D consortia*
- *R&D clubs and exchange of researchers*
- *Centre for Advanced Technology*
- *Patenting and licencing activities*

And to the world of science through:

- *Publication activities*
- *Network co-operation*
- *PhD education and post docs*

Risø-R-894(EN)
ISBN 87-550-2180-8
ISSN 0106-2840

Available on request from:
Information Service Department
Risø National Laboratory
P.O. Box 49, DK-4000 Roskilde, Denmark
Phone +45 46 77 46 77, ext. 4004/4005
Telex 43116, Fax +45 46 75 56 27
http://www.risoe.dk
e-mail: risoe@risoe.dk

Key Figures

Risø has a staff of more than 900, including more than 300 researchers and 100 PhD students and post docs. Risø's 1996 budget totals DKK 471 m, of which 45 % come from research programmes and commercial contracts, while the remainder is covered by government appropriations.